Chemical Engineering Journal 471 (2023) 144675

Contents lists available at ScienceDirect

Chemical Engineering Journal

journal homepage: www.elsevier.com/locate/cej

Stretchable, self-healing, biocompatible, and durable ionogel for continuous wearable strain and physiological signal monitoring

Katherine Le [a,c,*,1], Xia Sun [b,*,1], Junjie Chen [d], Johnson V. John [d], Amir Servati [a,c], Hossein Heidari [d,e], Ali Khademhosseini [d], Frank Ko [a], Feng Jiang [b], Peyman Servati [c,*]

[a] Advanced Fibrous Materials Laboratory, Department of Materials Engineering, University of British Columbia, V6T 1Z4, Canada
[b] Sustainable Functional Biomaterials Laboratory, Department of Wood Science, University of British Columbia, Vancouver, BC V6T 1Z4 Canada
[c] Flexible Electronics and Energy Lab, Department of Electrical and Computer Engineering University of British Columbia, V6T 1Z4, Canada
[d] Terasaki Institute for Biomedical Innovation, Los Angeles, CA 90024, USA
[e] School of Engineering and Materials Science, Queen Mary University of London, London E1 4NS, United Kingdom

ARTICLE INFO

Keywords:
Electronic textiles
Ionic liquid
Ionogel
Self-healing
Physiological monitoring
Strain sensing

ABSTRACT

Electronic textiles (e-textiles) have great potential for use in wearable systems worn next to skin for continuous physiological monitoring, owing to their flexibility and conformability to the body. However, challenges exist in the long-term functionality and durability of these materials. This work presents a highly stretchable, self-healing, and biocompatible chloride-based ionogel fabricated from polymerization of thioctic acid, and 1-n-Butyl-3-methylimidazolium chloride ([BMIM]Cl) ionic liquid. With its adaptable mechanical properties and tunable viscosity by simple dilution, the ionogel precursor can be either cast into an ionogel film used for strain sensing applications up to 500% strain, or directly sprayed as a coating for e-textile electrodes for biopotential signal monitoring. The ionogel can reform at room temperature, demonstrating 73.5% stress recovery, and 84.8% modulus recovery after a 30-minute healing period. When used as a spray barrier coating on e-textiles, the ionogel displayed high resistance to abrasion, and reformed after adding ethanol to the surface. The electrical properties of the ionogel coated e-textiles satisfies the performance range desired for textile sensing electrodes. Further development and application of this ionogel material system can address long-term durability concerns by extending the usable lifetime of the sensors for wearable applications.

1. Introduction

E-textiles functionalized with electrically conductive or active materials have many applications in biological signal monitoring, environmental sensing, energy generation, and electromagnetic shielding. These materials must retain their functional properties and performance during use, and in the long term, provide reliable measurements within the systems they are incorporated in. Exposure to use conditions that involve stretching, bending, abrasion, and stability can impact material properties and performance. Specific to sensing electrodes used next-to-skin, consideration of durability is an important factor for long-term reliability and use, particularly for sensors intended for continuous monitoring. Currently, sensing electrodes used for biopotential signal monitoring are often fabricated from metals paired with metallic salts (i.e., chlorides), which function by transducing ionic current (i.e., sodium, potassium, calcium, chloride ions) from the skin surface, into electron current, through metallic wires of a given recording system/instrument. Disposable gel-type Ag/AgCl electrodes are mostly used in biopotential signal monitoring in clinical settings. However, these electrodes are not suitable for repeated and long-term use, as the gel electrolyte material dries out over time. Electrodes made from conductive metals, polymer films, or coated textiles are commonly used. However, owing to the absence of an electrolyte layer, and low contact or adhesion to the skin, they tend to have a higher sensitivity to motion artifacts, produce fluctuations in potential, and cause signal distortion over time. While distortions in signal features may be corrected by signal processing methods, it is more ideal to develop materials with polarization potential stability over time, to ensure minimal interference with the collected

* Corresponding authors at: Flexible Electronics and Energy Lab, Department of Electrical and Computer Engineering University of British Columbia, V6T 1Z4, Canada(Katherine Le,Peyman Servati).
E-mail addresses: lekather@student.ubc.ca (K. Le), xiasun@mail.ubc.ca (X. Sun), peymans@ece.ubc.ca (P. Servati).
[1] Shared co-first authorship

https://doi.org/10.1016/j.cej.2023.144675
Received 20 April 2023; Received in revised form 16 June 2023; Accepted 6 July 2023
Available online 11 July 2023

signal. Encapsulation and protective barrier coatings including thermoplastic polyurethane (TPU), polyethylene, polyimide, silicone, epoxy resin, or polydimethylsiloxane of e-textiles can offer protection to the functionalized materials, enabling long-term use, with several studies that have examined the change in resistance and sensing properties after washing cycles [1–7]. The main challenges in the context of next-to-skin sensing electrode applications include the balance in maintaining the electrical conductance and performance of the material with the added protective barrier, flexibility, and moisture permeability of the textile, which can impact the wear and comfort properties.

High-performance supramolecular polymer networks have garnered significant interest in recent years due to their unique properties and potential applications in various fields. Thioctic acid (TA, or lipoic acid) is a naturally occurring molecule found in animals, functioning as a cofactor for important mitochondrial enzyme effects in metabolic systems [8]. Significant work by Zhang et al. demonstrated the synthesis and properties of a dynamic supramolecular polymer network based on TA comprising two types of dynamic chemical bonds in the compound: a covalent disulfide bond and a noncovalent hydrogen bond of its carboxyl group [9]. The polymer network was formed via ring-opening polymerization, imparting high stretchability, strength, moldability, and self-healing properties. The addition of other compounds has been demonstrated to further strengthen the cross-linked network by replacing weak hydrogen bonds, enhancing the material's overall performance. Subsequent studies by the group showcased the high structural order, tunable properties, and recyclability of thioctic acid-based supramolecular networks, applied as adhesives for dry and wet environments, smart sensing, and ion-transport materials [10–14]. Recent devlopments in thioctic/lipoic acid-based materials have included a wide range of application areas: the incorporation of poly-lipoic nanoparticles as biocompatible nanovectors in tissues [15], ionic conductor paints and films for stretchable and healable electronic materials through the automous polymerization of thioctic acid [16], a self-repairable epoxidized natural rubber/poly(lipoic acid) elastomer [17], and anti-bacterial/oxidation, and self-healing polyTA-based coating for magnesium alloy stents [18]. Therefore, there is high potential for utilizing polyTA materials in wearable textiles for achieving fanscinating properties.

Ionic liquids (IL) consist of organic/inorganic cations and anions with many benefits including low melting temperatures, good ionic conductivity, high thermal and chemical stability, tunable physical and chemical properties. They have been applied in various areas [7,19–21] such as sensors, actuators, solvents in chemical processes, energy devices including batteries and fuel cells, and biological processes in pharmaceutics and biomedicine [21–26]. ILs have been polymerized into ionogel used as quasi-solid-state electrolytes, strain sensors for movement detection [16,22,27,28], and reported in cutaneous electrode applications for biological sensing, specifically for improving skin contact, and maintaining low contact impedance with skin [19,27,29–32]. By combining ionic liquid and polyTA materials, a new type of ionogel is proposed and fabricated, which contributes to the design of next-to-skin sensing electrode applications, while also maintaining the desired electrical conductance and performance of the material.

In this work, a novel stretchable, self-healing, biocompatible, and chemically recyclable chloride-based ionogel with sensing and physiological monitoring capabilities is presented. The ionogel is prepared using TA and [BMIM]Cl, dissolved in ethanol. [BMIM]Cl ionic liquid has been used as a biocompatible stabilizer of proteins and enzymes in biopharmaceuticals and drug delivery systems [33,34], ionic electroactive films for muscle tissue engineering [24], as well as additives in cosmetic formulations used for skin and hair cleansing [35]. The ionogel is demonstrated as a standalone ionically conductive material for strain sensing applications, and a functional and self-healing protective electrolyte coating layer for e-textile sensors used for biopotential signal monitoring. The functional and adaptive properties of the material enable good skin-electrode contact, thereby lowering contact impedance, while the healing properties have the potential to extend the durability of coated textile sensors for long-term use. The versatility of this material addresses both functional and durability aspects that are critical for the adoption and long-term use of e-textile materials in sensing and physiological applications.

2. Materials and methods

2.1. Materials

Thioctic acid (TA, or α-lipoic acid), 98.0% was obtained from Tokyo Chemical Industry (TCI America). 1-n-Butyl-3-methylimidazolium chloride, ≥98.0% ([BMIM][Cl]) and ethanol were obtained from Sigma-Aldrich. Polyurethane (PU) pellets (Texin® 285A) were obtained from Covestro AG. *N,N*-Dimethylformamide (DMF) was purchased from Sigma-Adrich. Silver coated (99.9%) plain woven nylon fabric (Bremen, Statex, Germany) was obtained from VTTech Textiles (USA).

2.2. Preparation of pTA gel

The preparation of pTA ionogel was based on an evaporation-induced polymerization process. Namely, 3 g of TA monomer was dissolved in 30 mL ethanol, and 0.507 g [BMIM][Cl] (molar ratio to TA: 1:5) was added. After stirring, a clear and transparent yellow TA solution was obtained (Fig. S1a). Then, the solution was poured into a rectangular mold and vacuum degassed to remove entrapped air bubbles before curing. The mold with TA solution was placed at room temperature for 3 days to allow for complete evaporation of ethanol, after which transparent pTA ionogels were formed (Fig. S1b).

Separate pTA-IL solutions were prepared for spray coating on conductive silver-nylon (Ag-nylon) plain weave fabric (Fig. S1c). An airbrush system at 690 kPa was used to spray the coatings onto the fabric. A solution containing 1% PU-DMF was prepared and coated onto the fabric to provide a thin and protective layer of the metallic coating, and to lower the surface energy for better adhesion for the subsequent spraying of the pTA-IL layer.

2.3. Mechanical properties

The tensile mechanical properties of pTA ionogels were measured on an Instron machine (Instron 5969) with a load cell of 500 N and a crosshead speed of 50 mm/min. The samples were cut into rectangular shapes (fixture length: 10 mm, width: 5 mm, thickness: ~0.4 mm). For cyclic tests, the sample was stretched to a fixed strain (50%, 100%, 200% and 300%) for different cycles. For energy dissipation tests, the sample was stretched to different strains (50%, 100%, 200% and 300%). The toughness (W, kJ/m^3) was calculated by integrating the area under the stress–strain curves, while the dissipated energy was calculated by integrating the area between the loading curve and unloading curve.

2.4. Conductivity and strain sensitivity tests

The conductivity was measured on an electrochemical workstation (Gamry Interface E, Gamry Instruments Inc). The ionogel sample ($S = 1.76\ mm^2$, thickness ≈ 0.4 mm) was sandwiched between a pair of stainless-steel electrodes ($S = 1.76\ mm^2$, thickness = 1 mm) and the resistance was obtained from the intercept of the x-axis of the electrochemical impendence spectroscopy (EIS) Nyquist plot from 10^6 to 10 Hz. The conductivity (σ, mS/m) was calculated by $\sigma = d/R^*A$, where d was the distance between two electrodes, R was the resistance and A was the contact area between electrodes and ionogel.

The strain sensitivity was tested by combining the Instron machine and a digital source meter (Keithley 2450). The ionogel sample was fixed on the Instron machine connected with the source meter through copper wires, and when the sample was stretched, the real-time resistance change ($\Delta R/R_0$) was recorded by the source meter. The $\Delta R/R_0$ of

different strains and the cyclic performances were examined.

2.5. Bending characterization

Bending properties of the ionogel coated and bare Ag-nylon woven fabrics were compared through characterization of bending rigidity and hysteresis (recoverability of textile). The KES-FB20S bending tester (Kato Tech, Japan) and software (KES-FB Measurement Program, Version 8.07, Japan) were used to measure these characteristics. For each test, the bending moment–curvature curves were plotted, and bending rigidity and hysteresis were calculated. The measurement sensitivity was 0.49 N*cm (machine units: 50 gf*cm), bending displacement velocity was 0.5 cm^{-1}/s, and bending curvature was 2.5 cm^{-1}. Bending rigidity describes the fabric resistance to bending and is defined as the first derivative of the moment–curvature plot [36]. Bending hysteresis is the energy loss within a bending cycle when a fabric deforms and recovers, and is calculated as the difference in bending moment from the loading and unloading plot at a fixed bending curvature [36]. Lower values for bending rigidity and hysteresis indicate that the fabric has low rigidity and good recoverability. The bending tests for the uncoated and coated Ag-nylon plain weave fabrics (L:10 cm, W:4 cm; 3 measurements per fabric, n = 3) were measured, with fabrics rotated through to allow the material to recover after each trial.

2.6. Field emission scanning electron microscopy (FE-SEM)

FE-SEM (Zeiss Sigma, Germany) was used to observe ionogel film coated on the conductive textile (secondary electron signal, 10 kV accelerating voltage, 8 mm working distance). Micrographs of the coated textile surfaces were taken after the coating process, after mechanical abrasion, and after ethanol was applied to the abraded textile surface to demonstrate the self-healing process.

2.7. Electrochemical impedance spectroscopy

Electrical impedance spectroscopy (EIS) was performed on the skin phantom, using a three-electrode measurement setup. The Ag-nylon woven fabric spray coated with the ionogel was the working electrode (WE), and sintered Ag/AgCl electrodes served as counter (CE) and reference (RE) electrodes. The WE and CE were placed 5 cm apart, and WE and RE were 1 cm apart (Fig. S2a) on a skin phantom (S.1, Fig. S3). The results for the ionogel coated fabrics were compared with uncoated Ag-nylon woven fabric and sintered Ag/AgCl electrodes tested as WEs. The EIS scans were performed using an electrochemical workstation (BioLogic VMP 300, France), in potentiostatic mode, in which a sinusoidal voltage of 1 V was applied, using a frequency scan from 10 kHz to 0.1 Hz, with 10 points per decade, and three measurements per reading. Analysis of the measurements was performed by comparing impedance values at frequency points of interest, and equivalent circuit modeling to calculate circuit component parameters. The Simplified Randles circuit was selected to represent the skin-electrode interface and used for impedance estimation [37]. The model comprises a resistor R_s in series with a parallel resistor (R_d) and capacitor (C_d) (Fig. S2b). R_s represents the total resistance of the skin, wires and electrodes, the capacitor C_d represents the electrical charge between the electrode and skin, R_d represents the resistance between skin and electrode during the charge transfer process [38].

2.8. Self-Healing properties

The self-healing properties were explored by performing tensile tests. An ionogel specimen (length: 20 mm, width: 5 mm, thickness: ~0.4 mm) was cut into two pieces, then the two pieces were combined immediately. Three different healing time periods were investigated (0.5 h, 2 h and 24 h, respectively), after which the ionogel was subjected to tensile tests with the same test procedure as the mechanical tests.

2.9. Biopotential signal monitoring

ECG was measured using a clinical 1-lead ECG system (Thought Technology Ltd., Canada), with a sampling rate of 2048 samples/sec., and comprising a data acquisition and processing software (Biograph Infiniti). Signals were collected from two channels simultaneously to compare the performance of the ionogel coated e-textile electrodes with the standard Ag/AgCl gel electrodes. A schematic of the electrode construction is shown in Fig. 1c (Fig. S4d). The sets of electrodes were attached side-by-side on the chest, following the manufacturer's guideline (Fig. S4a/1d). To note, the simultaneous recordings do not produce identical ECG signals, as they will pick up slightly different phase and amplitude differences due to relative positioning. The e-textile electrodes were attached to the skin using a snap clip connector compatible with ECG snap leads, and secured with medical tape (3M, USA). Six-minute test sessions with three trials for each electrode set were performed in a stationary seated position. The signals were compared visually, and average inter-beat intervals (IBI) were compared. In the frequency domain, the power spectral density plots were compared.

EMG recordings were collected using the same clinical system (Thought Technology Ltd., Canada) at a sampling rate of 256 samples/sec. Signals were simultaneously collected from two channels to compare the performance of the ionogel coated textile electrode, with the standard Ag/AgCl gel electrodes. The sets of electrodes were attached to the middle bicep (Fig. S4b). The simultaneous recordings do not produce identical EMG signals since they will pick up slightly different signals due to their relative positioning on the muscle. The e-textile electrodes were attached to the skin using a snap clip connector compatible with the EMG snap leads, and secured with medical tape (3M, USA). The EMG signals were compared by visual observation of the raw signal, based on the flexion and extension movements during the recording (Fig. S5), and power spectral density in the frequency domain was analyzed.

3. Results and discussion

3.1. Fabrication and characterization of pTA ionogel

Although electronic textiles have been widely investigated in recent years, challenges in their widespread adoption include the lack of durability and reliability of sensors and collection systems. Other important considerations related to e-textile electrode design include good conformability and biocompatibility between the electrode and skin during long-term use. Inspired by recent developments of ionogels and their fascinating properties such as ionic conductivity, modulus, cutaneous compatibility, and reusability [39–41], this work presents a novel ionogel that can be used either as a standalone cast film or coated on the e-textiles for continuous physiological monitoring. As shown in Fig. 1a, the ionogel was prepared by an evaporation induced polymerization process. The process involves the dissolving of thioctic acid (TA) and ionic liquid ([BMIM][Cl]) in ethanol. Upon evaporation of ethanol, the disulfide bonds on the TA rings undergo ring-opening polymerization, forming polythioctic acid (pTA) ionogel, as shown in Fig. 1b. X-ray diffraction (XRD) results also indicated the successful formation of ionogel, which indicated that the crystalized TA has been converted to amorphous pTA (S.2, Fig. S6). Differential scanning calorimetry (DSC), attenuated total reflectance-FTIR (ATR-FTIR) spectra and UV–Vis spectra were also employed to further indicated the successful preparation of pTA ionogel as shown and discussed in Fig. S7. More interestingly, the resulting ionogel can be diluted to any concentration and is adjustable over a wide range.The ionogel can be reused, spray-coated on a substrate or cast into a film (Fig. S1b–d). The adaptability and skin-mimetic mechanical properties of the pTA ionogel materials, self-healing ability, and strain sensitivity from the ionic liquid offer potential for use in next-to-skin physiological monitoring applications. These

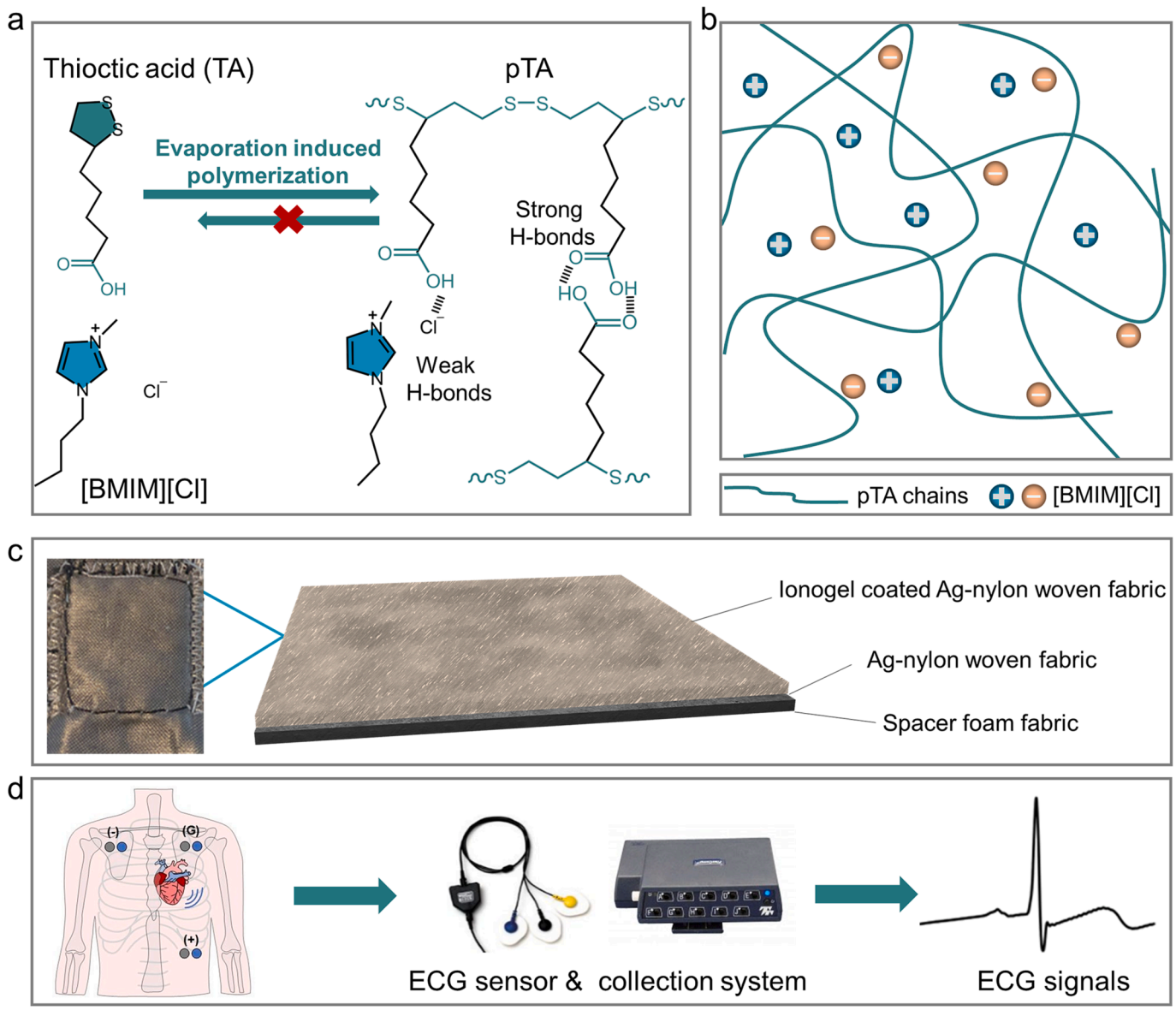

Fig. 1. Schematic illustration of pTA ionogel. (a) Schematic preparation process of pTA ionogel. (b) Schematic illustration of pTA ionogel. (c) Photo and schematic illustration of pTA ionogel coated textiles. (d) Schematic illustration of ECG monitoring process.

properties were leveraged, with the material prepared as a film used for strain sensitivity measurements, and spray coated on conductive fabric (Fig. 1c) to serve as an electrolyte material for electrodes used in bio-potential signal monitoring (ECG application shown in Fig. 1d).

3.2. Mechanical properties

The pTA ionogel exhibited good mechanical and self-healing properties due to the reconstruction of dynamic S-S bonds. The mechanical properties of pTA ionogel were measured by tensile tests, with a representative stress–strain curve shown in Fig. 2a. The ionogel showed a high strain of 721.3 ± 80.4% and a tensile strength of 0.090 ± 0.003 MPa, due to the dynamically crosslinked network. The ionogel also displayed a moderate modulus of 0.158 ± 0.002 MPa comparable to human skin (25–220 kPa) [42], which is beneficial for human–machine interface and wearable electrode applications. Fig. 2b shows the ionogel samples in the tensile machine under a high strain.

Energy dissipation behavior was investigated as shown in Fig. 2c,d. It is obvious that with an increase in external strain, the dissipated energy increases, which indicates that more S-S bonds and physical interactions are broken during stretching. For example, when the strain was 50%, the dissipated energy was 1.84 kJ/m^3, while at 300% strain, the dissipated energy increased to 57.8 kJ/m^3. Under low strain, the S-S bonds as well as the abundant hydrogen bonds can quickly reform after deconstruction, while under high strain, these dynamic covalent bonds or physical interactions cannot completely recover, thereby inducing a higher dissipated energy. Moreover, the reversible S-S bonds and hydrogen bonds endow the ionogel with durability and self-healing properties. Fig. 2e displays curves for the 85 cycles of stretching and releasing under 50% strain. Apart from the first cycle, the subsequent cycles nearly overlap, with a minor decrease, suggesting that the ionogel has high elastic recovery. The maximum tensile stress during each cycle was recorded and shown in Fig. 2f. During the process, the maximum tensile strength only decreased from 0.044 to 0.032 MPa (remaining 73% of the first cycle). In the last few cycles, the maximum tensile strength remained nearly constant.

To further demonstrate the durability of the pTA ionogel, more cyclic tests were carried out under different strains (100%, 200% and 300%, respectively) as shown in Fig. S8a–f. Similarly, the ionogel still showed overlapping curves under different strains, indicating excellent

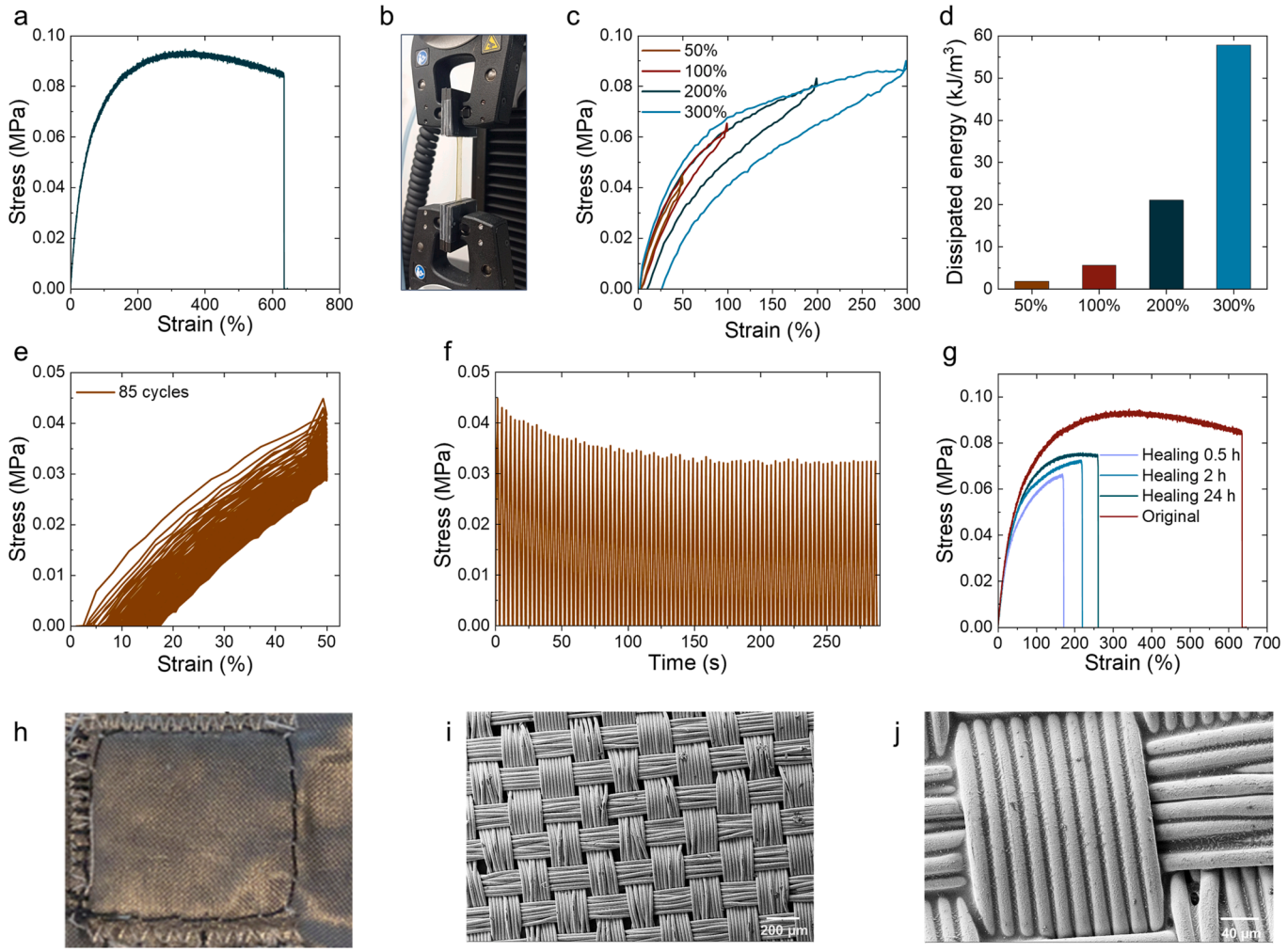

Fig. 2. Mechanical properties and self-healing properties. (a) Stress–strain curve of pTA ionogel. (b) Digital photo of pTA ionogel under stretching. (c) Cyclic stretching-releasing stress–strain curves under different strains and (d) the corresponding dissipated energy. (e) Stress–strain curves of 85 cycles under 50% strain and (f) the corresponding maximum tensile stress. (g) Stress-Strain curves of pTA ionogel after different healing time. (h) Photo of ionogel coated textile. SEM micrographs of ionogel film spray coated onto Ag-nylon plain weave textile (i) 55x and (j) 300x.

durability. The tensile tests also measured self-healing properties, and the stress–strain curves under different healing periods are presented in Fig. 2g. With the prolonged healing time, the tensile strength, modulus (Fig. S9), strain and toughness (Fig. S10) were gradually recovered due to the reconstruction of S-S bonds and hydrogen bonds at the healing interface. After 30 min of healing, the stress could recover 73.5%, while the modulus could recover 84.8%, revealing a fast and highly efficient healing process. Although the strain and toughness showed a relatively low healing efficiency due to the stress concentration at the interface, this stretchable and durable ionogel demonstrates high potential for healable coatings in cutaneous electrode applications. Further improvements to the self-healing properties can be made by heating the material above the transition temperature of 52 °C to thermally activate the dimeric H-bonds in the pTA structure [16]. Wang et al. demonstrated that after heating a fractured pTA-1-ethyl-3-methylimidazolium ethyl sulfate ([EMI][ES]) ionogel specimen at 55 °C for 6 h, the material almost recovered its original tensile strength and elongation values [16]. More importantly, the pTA ionogel can be dissolved in ethanol, which serves as the basis for preparing the ionogel coating. Fig. 2h shows the ionogel coated e-textile electrode. SEM micrographs of the spray-coated ionogel film on Ag-nylon woven fabric are displayed in Fig. 2i,j. The images and thickness measurement (0.073 ± 0.013 mm, Table S1) show that the ionogel material is uniformly incorporated between the fibres and across the surface of the fabric.

3.3. Electrical characterization

3.3.1. Ionic conductivity & sheet resistance

With the addition of the ionic liquid, the ionogel exhibits considerable ionic conductivity, which is advantageous in sensing electrode applications, specifically in serving as an electrolyte coating. As shown in Fig. 3a,b, the Nyquist plot consists of two regions, the low-frequency region, which indicates the capacitive characteristics, and the high-frequency region (arc region) related to the equivalent series resistance (ESR) of the electrolyte [43]. The form of the curve shows low ESR due to the fast transport of charge carriers at electrode–electrolyte interface, indicating that the Cl^- ions of the ionic liquid can facilitate high transport in the ionogel electrolyte, and diffuse to the surface of electrodes. The ionic conductivity was calculated as 2.27 ± 0.23 mS/m, and comparable to some reported ionogels [44,45].

Sheet resistance was measured for the ionogel film and coated Ag-nylon textile (0.176 ± 0.007 Ω/sq.). The experimental method is summarized in S.3. The sheet resistance of ionogel film was measured to be 0.120 ± 0.012 Ω/sq. The ionogel coated Ag-nylon textile was 0.248 ± 0.010 Ω/sq. Results are summarized in Table S2.

3.3.2. Electrical impedance spectroscopy (EIS)

EIS results for the ionogel coated Ag-nylon textile were measured and compared with bare Ag-nylon textile, and standard gel electrodes

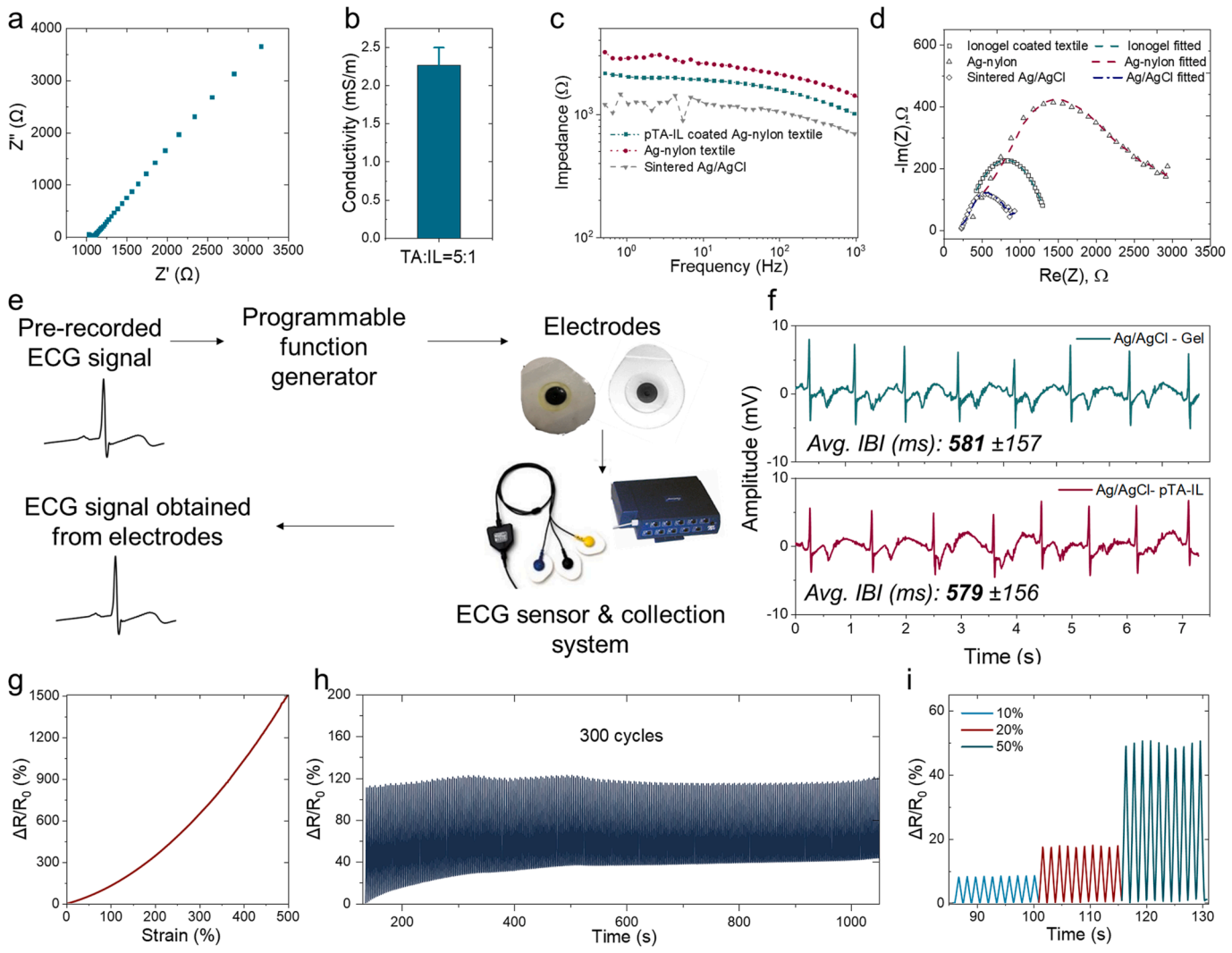

Fig. 3. Electrical Characterization of ionogel and ionogel coating. (a) Nyquist plot of ionogel and (b) corresponding ion conductivity. (c) Example Bode plots displaying impedance vs. frequency for uncoated, coated ionogel Ag-nylon fabrics, and sintered Ag/AgCl electrodes (d) Example Nyquist plots with measured and fitted data for uncoated, coated ionogel Ag-nylon fabrics, and sintered Ag/AgCl electrodes. (e) Schematic of experimental design to measure pre-recorded ECG signal from electrodes. (f) ECG signal obtained from Ag/AgCl-gel and Ag/AgCl-ionogel electrodes. (g) $\Delta R/R_0$ versus strain (0–500%). (h) $\Delta R/R_0$ under 100% strain for 300 cycles. $\Delta R/R_0$ under different strains (i) 10%, 20% and 50%;

using the prepared skin phantom (S.1, Fig. S2–S3). Estimates for the components of the skin-electrode impedance model applied the simplified Randle's circuit (Fig. S2b), and R_s, R_d, and C_d were calculated in MATLAB (R2022a, Mathworks) using a parameter modelling approach and least squares nonlinear curve fitting method. Example results showing the Nyquist and Bode plots from the measurements are presented in Fig. 3c,d and summarized in Table 1.

Model parameters were estimated from the following equations:

Table 1
Summary of average impedance results at 1 Hz, 10 Hz, 145 Hz, and estimates of circuit model parameters for electrode materials investigated.

	Z @ 1 Hz [kΩ]	Z @ 10 Hz [kΩ]	Z @ 145 Hz [kΩ]	Rs [kΩ]	Rd [kΩ]	Cd [F]
Ionogel + Ag-textile	1.70	1.58	1.27	0.38	1.25	7.93x10^{-8}
Ag-nylon textile (bare)	2.86	2.84	2.22	0.59	2.34	1.64x10^{-8}
Ag/AgCl sintered electrode	1.35	1.10	0.87	0.21	0.89	9.85x10^{-8}

$$Z = R_s + \frac{R_d}{(1+X_d^2)} - j\frac{R_d X_d}{(1+X_d^2)} \tag{1.1}$$

$$where\ X_d = R_d C_d . \omega \quad \omega = 2\pi f \tag{1.2}$$

$$|Z|^2 = A^2 + B^2 \tag{2.1}$$

where the real and imaginary components of $|Z|$ as A and B are:

$$A = R_s + \frac{R_d}{(1+X_d^2)} \tag{2.2}$$

$$B = -\frac{R_d X_d}{(1+X_d^2)} \tag{2.3}$$

Overall, the results for all electrode materials tested fall within the same order of magnitude and range (Table 1). The reference Ag/AgCl sintered electrodes have the lowest impedance, estimated resistance and capacitance values overall, closely followed by the Ag-nylon textile coated with the ionogel film, while the uncoated Ag-nylon textile has the highest overall measured and estimated values (Fig. 3c,d). The results show that the addition of the ionogel coating to the Ag-nylon fabric

lowers the impedance and resistance at the skin-electrode interface through providing a medium for ionic to electron current transfer. Furthermore, an additional metallic salt coating of AgCl onto the Ag-textile is thought to further lower impedance and resistance. The electrode impedance of the ionogel coated Ag-nylon textile meets desired performance criteria for use in electrocardiogram signal measurement, with values lower than 1 MΩ (1–5 MΩ in 5–100 Hz range) [46–48]. In addition, the impedance results of the ionogel coated e-textile from this work have been compared to other studies that have utilized ionic liquid coating for e-textile electrode applications and are found to be within close range or lower than reported results (Table 2), which demonstrates their suitability for biopotential signal monitoring.

3.3.3. Recording of simulated ECG signal

Ag/AgCl electrodes coated with the ionogel film, and a set of reference Ag/AgCl gel electrodes were used to measure a pre-recorded ECG signal from a programmable function generator (S.4). The signal collected from the electrodes was compared visually. The average inter-beat interval (milliseconds) was compared between the two readings (Fig. 3e). The signals presented in Fig. 3f show both electrodes could read the ECG signal, with waveform morphology and inter-beat intervals (IBI) of similar quality. In both signals, instances of baseline drift in the signal are present between 1.5, 5.0, and 6.5–7.0 s. The preliminary results indicate that the ionogel coated electrode enables the collection of an acceptable quality ECG or biopotential signal from the body.

3.3.4. Strain sensitivity

Incorporating the [BMIM]Cl ionic liquid softened and stabilized the pTA network and induced considerable ionic conductivity to the ionogel material. Therefore, under external strains, the change in geometry of the ionogel induces the ion transport channels, which result in the resistance changes, and thus demonstrates the potential for the pTA ionogel to be used in strain sensor applications. A change in geometry via stretching can induce ion conduction in the materials for amorphous polymer electrolytes or ionic conductors under external strains. Specifically, the polymer chains opening or moving enhances ion conduction by creating more coordination sites [49–52]. This results in a change in the material's resistance. The strain sensitivity of the pTA ionogel was tested under various strain scenarios and cycling, by combining resistance measurements (Keithley) with strain cycling (Instron). As shown in Fig. 3g, the relative resistance change ($\Delta R/R_0$) was increased monotonically with the increase in external strain. When the strain was 500%, the $\Delta R/R_0$ increased to 1507%, showing a very high sensitivity. Gauge factor (GF) was employed to determine the strain sensitivity, which was calculated as $(\Delta R/R_0)$/strain, and the result is presented in Fig. S11a. The GF also increased with the applied strain, and when the strain was 500%, the GF was 3.01, which was superior to many reported ionogels as shown in Fig. S12 in terms of the sensing range and the GF. Impressively, the conductivity and strain sensitivity of the pTA ionogel was still maintained. As shown in Fig. S13, the healed sample revealed a conductivity of 2.26 ± 0.21 mS/m, corresponding to a high self-healing efficiency of 99.5%, and a GF of 1.58 at 200% strain, indicating a high self-healing efficiency of 91.9%. Considering the durability of the ionogels revealed by the cyclic tensile tests for 300 cycles under 100% strain, (Fig. 3h) it is expected that the ionogel would exhibit high stability after cyclic tensile loading and stretching, with a highly stable and repeatable signal. The slight baseline shift was ascirbed to the fact that the fully-physically crosslinked network could not fully recover after deformation. This suggests that the ionogel can be used to sense different external strains (Fig. 3i, Fig. S11c) with high sensitivity (detection limit, 1%, Fig. S11b). More importantly, even after 2 weeks storage, the pTA ionoel still showed stable conductivity, the same sensing range as well as comparable strain sensitivity (GF = 2.9 at 500% strain, Fig. S14), thereby demonstrating the long-term stability and durability of the pTA ionogel. Based on the results presented, the pTA ionogel shows high stability and sensitivity for strain sensor applications.

Table 2
Comparison of electrode impedance values for studies investigating IL coatings.

Material	Z [Ω], Frequency Range [Hz]	Ref.
Au + IL gel (EMISE + PEGDA) & PEDOT:PSS + IL gel (EMISE + PEGDA)	10^5-10^6 Ω, 0.1–10 Hz	[19]
PEDOT:PSS + IL gel (2-cholinium lactate methacrylate, cholonium lactate, PEGDA), 30-50 wt% IL	2–4 x10^4 Ω, 1–10 Hz	[31]
PEDOT:PSS + IL gel (EMISE, PEGDA, 2-benzoyl-2-propanol)	1–2 x10^5 Ω, 1–10 Hz	[29]
1. Carbon coating on textile + 2.5%, 5% IL (EMIM-TFSI)	1.1–3 × 10^3 Ω, 5 Hz	
2. PEDOT:PSS + 6.25% PDMS +2.5%, 5% IL (EMIM-TFSI)	2.20–30 Ω, 5 Hz	[30]
Ag-nylon plain weave fabric + PU-pTA-[BMIM]Cl IL	1–2 × 10^3Ω, 1–10 Hz	This work

3.4. Durability and biocompatibility

The bending properties were characterized to observe and quantify the change in flexibility of the ionogel coated e-textile (Fig. 4a). The bending moment versus curvature for one cycle is shown for both uncoated and coated Ag-nylon plain weave textiles tested (Fig. 4b). Results are summarized in Table 3. Lower values for bending rigidity and hysteresis indicate that the material is more flexible and has good recoverability. While the ionogel coating increases the overall bending rigidity and hysteresis substantially, the overall measured values for both e-textiles are very low as the fabrics are very thin. In comparison to results reported for a nylon plain weave textile substrate (thickness: 0.097 mm) for e-textile embroidery, the results are lower in comparison [53].

Ionogel-coated fabrics (unabraded specimen Fig. 2i,j) were abraded with a rotating fabric covered motorhead for approximately 30 s. The surface after abrasion is shown in Fig. 4c, which shows that the film remains tact with some displacement and agglomeration of the coating layer. To examine the effect of surface reformation and potential sanitizing method, approximately 1 mL of ethanol was added (dropwise) to the abraded textile surface. It is expected that the ethanol can allow for the redispersion of the displaced regions of the film. Fig. 4d shows the reformed surface after ethanol addition, in which the darker regions on the fabric structure are indicative of the abraded regions of the fabric. The visual observations indicate that the ionogel coating on the fabric can be redispersed and reformed after mechanical abrasion to the surface. Furthermore, both the surface coating and standalone film material can be recycled by dissolution in ethanol, heating to approximately 55 °C, above the transition temperature of 52 °C, to thermally activate the dimeric H-bonds in the polyTA structure, and be reformed into new ionic conductors, sensors, or adhesives [16,28].

Biocompatibility tests were performed to assess the suitability of the ionogel coated textile use for next-to-skin physiological signal measurements. The cell proliferation and viability test results (experimental methods described in **S.5**) demonstrate that the ionogel coated fabric is biocompatible with human dermal fibroblast cells after 12 and 24 h. Cell proliferation results in Fig. 4e,f show that the coated fabric is comparable to the control sample, and performs better than the standard reference gel electrolyte material. The cell viability (%) results (Figs. S15,16) show statistically similar results between the fabrics and gel electrolyte material after 12 h, with cell viability maintained for the fabrics after 24 h, while the viability for the gel electrolyte is reduced.

3.5. Biopotential signal monitoring – Electrocardiography (ECG) and electromyography (EMG)

Results for ECG and EMG recordings are displayed in Fig. 5. As shown in Fig. 5a&e, signals from disposable commercial electrodes and

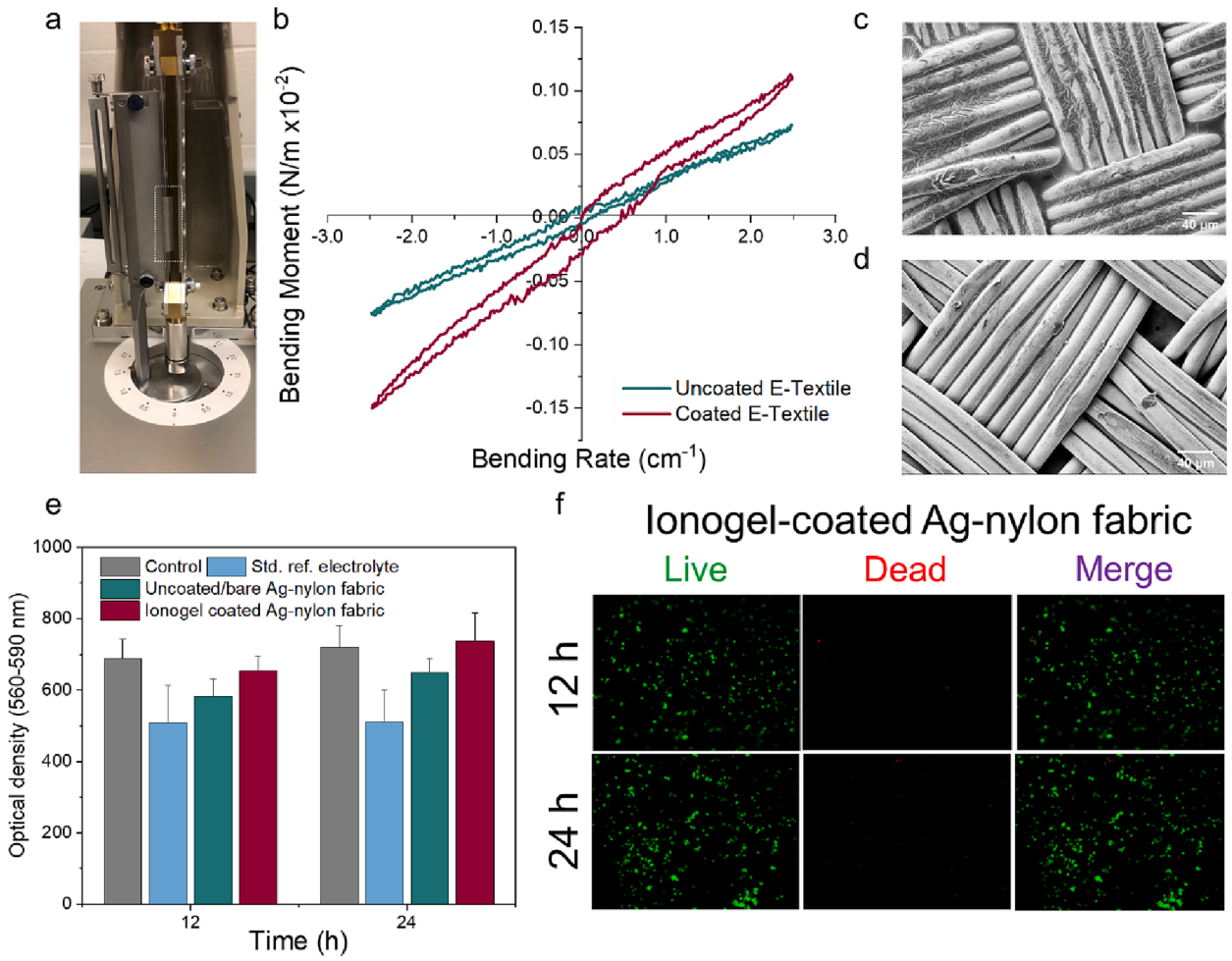

Fig. 4. Durability and biocompatibility. (a) Bending characterization: Fabric being tested in bending tester, KES-FB2-S. (b) Example bending moment vs curvature plot for uncoated and coated e-textiles. SEM micrographs of ionogel-coated fabric: (c) Abraded fabric (300x). (d) Abraded fabric after ethanol addition, showing regenerated film (300x). (e) Cell proliferation (optical density, 560–590 nm) on various substrates after incubation for 12 h and 24 h. (f) Live/dead assay fluorescent microscope images after 12 and 24 h (live cells shown as green, and dead cells as red). (For interpretation of the references to colour in this figure legend, the reader is referred to the web version of this article.)

Table 3
Summary of average bending rigidity and bending hysteresis for e-textiles and comparative nylon textile substrate.

	Bending Rigidity [10^{-4} Nm/m]	Bending Hysteresis [10^{-2} Nm/m]
Uncoated e-textile (0.052 mm thickness)	$2.73 \times 10^{-2} \pm 0.002$	$7.69 \times 10^{-3} \pm 0.0002$
Iongel coated e-textile (0.073 mm thickness)	$4.62 \times 10^{-2} \pm 0.001$	$1.43 \times 10^{-2} \pm 0.001$
Nylon textile (0.097 mm thickness)	$8.00 \times 10^{-2} \pm 0.001$	$5.37 \times 10^{-2} \pm 0.001$

the ionogel coated fabrics were recorded simultaneously. The ECG recordings show nearly identical signal quality between the two sets of electrodes from visual observation, with the same average inter-beat interval of 851 ± 49 ms, corresponding to approximately 70 beats/min. The amplitude for the ECG signal recorded by the textile electrode is slightly higher than the standard gel electrode (Fig. 5b); however, this does not impact the basic signal quality features (heartbeat and heart rate variability). Overall, the EMG recording from the two sets of electrodes show the same signal responses for bicep flexion and extension (Fig. 5f), with some observable differences in signal amplitude and noise. From the frequency domain periodograms (Fig. S17a,b), the signal power for both ECG and EMG of the ionogel coated textile electrodes is higher than the standard gel electrodes, with observable features visible in the low frequency band (0.03–0.2 Hz), indicative of the observed noise in the raw signals.

Signals were collected for two additional use cases: following a 24 h self-healing period (post abrasion and ethanol redispersion), and stability after 1 week of storage (Fig. 5c,d,g,h). For the ECG signals collected, a lower signal amplitude of the ionogel coated electrodes compared to the gel electrodes post-abrasion, following a 24 h healing period was observed (Fig. 5c). This is indicative of lower signal strength, given that the frequency analysis (Fig. S18) showed higher noise in the low frequency band (0.03–0.8 Hz) than the gel electrode. However, after the 1-week storage period, the ECG recording from the ionogel-coated electrode was observed return to the same amplitude range as the original recording (Fig. 5d&b). From all cases, the ECG signals collected (Fig. 5c,d) show the same average inter-beat interval calculated from two sets of electrodes tested. For both use cases tested, the EMG signals collected showed the same signal responses for bicep flexion and extension (Fig. 5g,h).

Overall, the results show that the ionogel coated Ag-textile electrodes can measure biopotential signals, with good quality recordings demonstrated for both ECG and EMG. Basic features observed for both signals recorded showed comparable performance to standard Ag/AgCl gel electrodes.

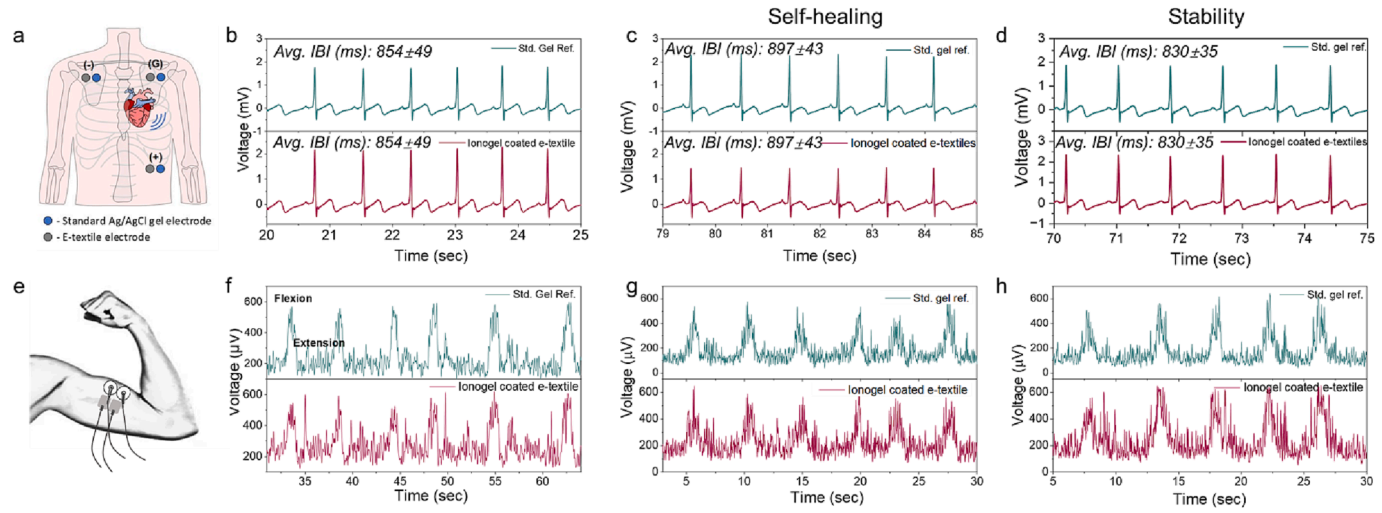

Fig. 5. Continuous physiological monitoring. (a) Schematic of ECG electrode placement. (b) Example simultaneous ECG signal recordings from standard reference electrodes and ionogel-coated Ag-nylon e-textile electrodes. (c) ECG signals obtained after self-healing (24 h healing period). (d) ECG signals obtained after 1-week of storage (ionogel electrodes). (e) Schematic of EMG electrode placement. (f) Example simultaneous EMG recordings from standard reference electrodes and ionogel-coated Ag-nylon e-textile electrodes. (g) EMG signals obtained after self-healing (24 h healing period). (h) EMG signals obtained after 1-week of storage (ionogel electrodes).

4. Conclusions

In this study, a stretchable, self-healing, biocompatible, and highly durable ionogel material prepared from [BMIM]Cl and TA has been demonstrated. The material has high adaptability in form, from cast and dilutable films to sprayable coatings for strain sensing and biopotential monitoring applications, respectively. The material demonstrated excellent self-healing capacity from being reformed at room temperature, with 73.5% stress recovery, and 84.8% in modulus recovery after a 0.5 h healing time. As a spray coated barrier on e-textiles, the ionogel demonstrated high resistance to abrasion, and was able to be reformed by the addition of ethanol to the surface. The material can be produced to various concentrations under room temperature condition, through the mixing of TA, IL, and ethanol, with highly adjustable mechanical properties. The ionogel (1:5 IL-TA concentration) demonstrated up to 721.3 ± 8.4% strain, 0.090 ± 0.003 MPa stress, and a modulus of 0.158 ± 0.002 MPa, indicating its suitability for cutaneous applications. The electrical properties of the ionogel coated e-textiles were measured, including sheet resistance (0.248 Ω/sq. ± 0.01) and skin-electrode impedance (below 2 kΩ from 0.1 to 1 kHz) demonstrating excellent performance, meeting specified properties, or within reported range of values for e-textile sensing electrodes. Strain sensitivity of the ionogel showed high stability under cycling loading at various strain levels, and a gauge factor of 3.0 at 500% strain. Results for biopotential signal recordings demonstrate that the Ag/AgCl ionogel-coated electrodes can read ECG signals, showing comparable quality to standard Ag/AgCl gel electrodes. Biocompatibility test results demonstrated that the ionogel coated fabrics are safe to use in next-to-skin applications for up to 24 h, with performance (cell proliferation and viability) exceeding that of the standard reference gel electrolyte material. Results for biopotential signal recordings demonstrate that the Ag/AgCl ionogel-coated electrodes can read and collect ECG and EMG signals, showing comparable quality to standard Ag/AgCl gel electrodes. The demonstrated functional and self-healing properties of the ionogel show great potential to extend the lifetime and enable continuous use of e-textile sensors. Future work should include long-term studies on the ionogel durability (varying thickness) as a strain sensor, and as a functional, protective coating for e-textile electrodes.

Declaration of Competing Interest

The authors declare that they have no known competing financial interests or personal relationships that could have appeared to influence the work reported in this paper.

Data availability

Data will be made available on request.

Acknowledgements

This work was supported by the Natural Sciences and Engineering Research Council of Canada (NSERC) Discovery and Alliance Grants, the Canada Foundation for Innovation (CFI), and the University of British Columbia (UBC) Four-Year Doctoral Fellowship. The author also thanks Pu Yang and Shawn Du from UBC for their help on ATR-FTIR test and DSC test, respectively.

Appendix A. Supplementary data

Supplementary data to this article can be found online at https://doi.org/10.1016/j.cej.2023.144675.

References

[1] S. Uz Zaman, X. Tao, C. Cochrane, V. Koncar, Understanding the washing damage to textile ECG dry skin electrodes, embroidered and fabric-based; set up of equivalent laboratory tests, Sensors (Switzerland) 20 (2020) 1272, https://doi.org/10.3390/s20051272.

[2] X. Liang, M. Zhu, H. Li, J. Dou, M. Jian, K. Xia, S. Li, Y. Zhang, X. Liang, M. Zhu, K. Xia, S. Li, Y.Y. Zhang, H. Li, J. Dou, M. Jian, Hydrophilic, breathable, and washable graphene decorated textile assisted by silk sericin for integrated multimodal smart wearables, Adv. Funct. Mater. 32 (2022) 2200162, https://doi.org/10.1002/ADFM.202200162.

[3] T. Linz, M. von Krshiwoblozki, H. Walter, P. Foerster, Contacting electronics to fabric circuits with nonconductive adhesive bonding, J. Text. Inst. 103 (2012) 1139–1150, https://doi.org/10.1080/00405000.2012.664867.

[4] K. Cherenack, C. Zysset, T. Kinkeldei, N. Münzenrieder, G. Tröster, Woven electronic fibers with sensing and display functions for smart textiles, Adv. Mater. 22 (2010) 5178–5182, https://doi.org/10.1002/ADMA.201002159.

[5] S. Wilson, R. Laing, E.W. Tan, C. Wilson, Encapsulation of electrically conductive apparel fabrics: effects on performance, Sensors (Switzerland). 20 (2020) 1–30, https://doi.org/10.3390/s20154243.

[6] X. Tao, V. Koncar, T.-H. Huang, C.-L. Shen, Y.-C. Ko, G.-T. Jou, How to make reliable, washable, and wearable textronic devices, Sensors (Switzerland). 17 (4) (2017) 673.

[7] M. Armand, F. Endres, D.R. MacFarlane, H. Ohno, B. Scrosati, Ionic-liquid materials for the electrochemical challenges of the future, Nature Mater 8 (8) (2009) 621–629.

[8] Linus Pauling Institute, Lipoic Acid, Oregon State Univ. (2023). https://lpi.oregonstate.edu/mic/dietary-factors/lipoic-acid.

[9] Q. Zhang, C.Y. Shi, D.H. Qu, Y.T. Long, B.L. Feringa, H. Tian, Exploring a naturally tailored small molecule for stretchable, self-healing, and adhesive supramolecular polymers, Sci. Adv. 4 (2018) 1–9, https://doi.org/10.1126/sciadv.aat8192.

[10] Q. Zhang, Y.X. Deng, H.X. Luo, C.Y. Shi, G.M. Geise, B.L. Feringa, H. Tian, D.H. Qu, Assembling a natural small molecule into a supramolecular network with high structural order and dynamic functions, J. Am. Chem. Soc. 141 (2019) 12804–12814, https://doi.org/10.1021/jacs.9b05740.

[11] Q. Zhang, Y. Deng, C.Y. Shi, B.L. Feringa, H. Tian, D.H. Qu, Dual closed-loop chemical recycling of synthetic polymers by intrinsically reconfigurable poly (disulfides), Matter. 4 (2021) 1352–1364, https://doi.org/10.1016/J.MATT.2021.01.014.

[12] Q. Zhang, D.H. Qu, B.L. Feringa, H. Tian, Disulfide-mediated reversible polymerization toward intrinsically dynamic smart materials, J. Am. Chem. Soc. 144 (2022) 2022–2033, https://doi.org/10.1021/JACS.1C10359.

[13] Y. Deng, Q. Zhang, C. Shi, R. Toyoda, D.H. Qu, H. Tian, B.L. Feringa, Acylhydrazine-based reticular hydrogen bonds enable robust, tough, and dynamic supramolecular materials, Sci. Adv. 8 (2022), https://doi.org/10.1126/sciadv.abk3286.

[14] C.-Y. Shi, D.-D. He, Q.i. Zhang, F. Tong, Z.-T. Shi, H.e. Tian, D.-H. Qu, Robust and dynamic underwater adhesives enabled by catechol-functionalized poly(disulfides) network, Natl. Sci. Rev. 10 (2) (2023), https://doi.org/10.1093/nsr/nwac139.

[15] J.W. Trzciński, L. Morillas-Becerril, S. Scarpa, M. Tannorella, F. Muraca, F. Rastrelli, C. Castellani, M. Fedrigo, A. Angelini, R. Tavano, E. Papini, F. Mancin, Poly(lipoic acid)-based nanoparticles as self-organized, biocompatible, and corona-free nanovectors, Biomacromolecules. 22 (2021) 467–480, https://doi.org/10.1021/acs.biomac.0c01321.

[16] Y. Wang, S. Sun, P. Wu, Adaptive ionogel paint from room-temperature autonomous polymerization of α-thioctic acid for stretchable and healable electronics, Adv. Funct. Mater. 31 (2021) 2101494, https://doi.org/10.1002/adfm.202101494.

[17] L. Kong, Y. Yang, M. Wu, X. Teng, Y. Wang, C. Xu, Design of epoxidized natural rubber/poly(lipoic acid) elastomer with fast and efficient self-healing under a mild temperature, Int. J. Biol. Macromol. 223 (2022) 446–457, https://doi.org/10.1016/j.ijbiomac.2022.11.040.

[18] Z.Q. Zhang, P.D. Tong, L. Wang, Z.H. Qiu, J.A. Li, H. Li, S.K. Guan, C.G. Lin, H. Y. Wang, One-step fabrication of self-healing poly(thioctic acid) coatings on ZE21B Mg alloys for enhancing corrosion resistance, anti-bacterial/oxidation, hemocompatibility and promoting re-endothelialization, Chem. Eng. J. 451 (2023), 139096, https://doi.org/10.1016/j.cej.2022.139096.

[19] P. Leleux, C. Johnson, X. Strakosas, J. Rivnay, T. Hervé, R.M. Owens, G. G. Malliaras, Ionic liquid gel-assisted electrodes for long-term cutaneous recordings, Adv. Healthc. Mater. 3 (2014) 1377–1380, https://doi.org/10.1002/ADHM.201300614.

[20] X. Liang, B. Qu, J. Li, H. Xiao, B. He, L. Qian, Preparation of cellulose-based conductive hydrogels with ionic liquid, React. Funct. Polym. 86 (2015) 1–6, https://doi.org/10.1016/J.REACTFUNCTPOLYM.2014.11.002.

[21] D.M. Correia, L.C. Fernandes, M.M. Fernandes, B. Hermenegildo, R.M. Meira, C. Ribeiro, S. Ribeiro, J. Reguera, S. Lanceros-Méndez, Ionic liquid-based materials for biomedical applications, Nanomaterials. 11 (9) (2021) 2401.

[22] S. Chen, H. Liu, S. Liu, P. Wang, S. Zeng, L. Sun, L. Liu, Transparent and waterproof ionic liquid-based fibers for highly durable multifunctional sensors and strain-insensitive stretchable conductors, ACS Appl. Mater. Interfaces. 10 (2018) 4305–4314, https://doi.org/10.1021/ACSAMI.7B17790/SUPPL_FILE/AM7B17790_SI_006.AVI.

[23] K. Kundu, B.K. Paul, S. Bardhan, S.K. Saha, Recent advances in bioionic liquids and biocompatible ionic liquid-based microemulsions,, Ion Liq. Surfactant Sci. Formul. Charact. Appl. (2015) 397–445, https://doi.org/10.1002/9781118854501.CH20.

[24] R.M. Meira, D.M. Correia, S. Ribeiro, P. Costa, A.C. Gomes, F.M. Gama, S. Lanceros-Méndez, C. Ribeiro, Ionic-liquid-based electroactive polymer composites for muscle tissue engineering, ACS Appl. Polym. Mater. 1 (2019) 2649–2658, https://doi.org/10.1021/ACSAPM.9B00566/SUPPL_FILE/AP9B00566_SI_001.PDF.

[25] N. Dib, C.M.O. Lépori, N.M. Correa, J.J. Silber, R.D. Falcone, L. García-Río, Biocompatible solvents and ionic liquid-based surfactants as sustainable components to formulate environmentally friendly organized systems, Polymers (Basel). 13 (9) (2021) 1378.

[26] N. Nikfarjam, M. Ghomi, T. Agarwal, M. Hassanpour, E. Sharifi, D. Khorsandi, M. Ali Khan, F. Rossi, A. Rossetti, E. Nazarzadeh Zare, N. Rabiee, D. Afshar, M. Vosough, T. Kumar Maiti, V. Mattoli, E. Lichtfouse, F.R. Tay, P. Makvandi, Antimicrobial ionic liquid-based materials for biomedical applications, Adv. Funct. Mater. 31 (2021) 2104148, https://doi.org/10.1002/ADFM.202104148.

[27] G.C. Luque, M.L. Picchio, A.P.S. Martins, A. Dominguez-Alfaro, N. Ramos, I. del Agua, B. Marchiori, D. Mecerreyes, R.J. Minari, L.C. Tomé, 3D printable and biocompatible iongels for body sensor applications, Adv. Electron. Mater. 7 (2021) 2100178, https://doi.org/10.1002/AELM.202100178.

[28] C. Dang, M. Wang, J. Yu, Y. Chen, S. Zhou, X. Feng, D. Liu, H. Qi, Transparent, highly stretchable, rehealable, sensing, and fully recyclable ionic conductors fabricated by one-step polymerization based on a small biological molecule, Adv. Funct. Mater. 29 (2019) 1902467, https://doi.org/10.1002/ADFM.201902467.

[29] S. Takamatsu, T. Lonjaret, D. Crisp, J.-M.-M. Badier, G.G. Malliaras, E. Ismailova, Direct patterning of organic conductors on knitted textiles for long-term electrocardiography, Sci. Rep. 5 (2015), https://doi.org/10.1038/srep15003.

[30] M. Alizadeh-Meghrazi, B. Ying, A. Schlums, E. Lam, L. Eskandarian, F. Abbas, G. Sidhu, A. Mahnam, B. Moineau, M.R. Popovic, Evaluation of dry textile electrodes for long-term electrocardiographic monitoring, Biomed. Eng. OnLine 2021 201. 20 (2021) 1–20. https://doi.org/10.1186/S12938-021-00905-4.

[31] M. Isik, T. Lonjaret, H. Sardon, R. Marcilla, T. Herve, G.G. Malliaras, E. Ismailova, D. Mecerreyes, Cholinium-based ion gels as solid electrolytes for long-term cutaneous electrophysiology, J. Mater. Chem. C. 3 (2015) 8942–8948, https://doi.org/10.1039/C5TC01888A.

[32] X. Fu, Y. Wang, W. Wang, D. Yu, Ionic liquid regenerated cellulose membrane electroless plated by silver layer for ECG signal monitoring, Cellulose. 29 (2022) 3467–3482, https://doi.org/10.1007/S10570-022-04487-9/FIGURES/10.

[33] C.D. Tran, T.M. Mututuvari, Cellulose, chitosan, and keratin composite materials, Controlled drug release, Langmuir. 31 (2015) 1516–1526, https://doi.org/10.1021/LA5034367/SUPPL_FILE/LA5034367_SI_001.PDF.

[34] M.G. Ventura, A.I. Paninho, A.V.M. Nunes, I.M. Fonseca, L.C. Branco, Biocompatible locust bean gum mesoporous matrices prepared by ionic liquids and a scCO2 sustainable system, RSC Adv. 5 (2015) 107700–107706, https://doi.org/10.1039/C5RA17314K.

[35] F. Giroud, Organic salt conditioner, organic salt-containing composition, and uses thereof, US20040005286A1, 2004. https://patents.google.com/patent/US20040005286 (accessed March 2, 2022).

[36] J.L. Hu, W.M. Lo, M.T. Lo, Bending hysteresis of plain woven fabrics in various directions, Text. Res. J. 70 (2000) 237–242, https://doi.org/10.1177/004051750007000310.

[37] S. Grimnes, Ø. Martinsen, Bioimpedance and bioelectricity basics, Elsevier (2015), https://doi.org/10.1016/C2012-0-06951-7.

[38] B. Taji, S. Shirmohammadi, V. Groza, I. Batkin, Impact of skin-electrode interface on electrocardiogram measurements using conductive textile electrodes, IEEE Trans. Instrum. Meas. 63 (2014) 1412–1422, https://doi.org/10.1109/TIM.2013.2289072.

[39] J. Le Bideau, L. Viau, A. Vioux, Ionogels, ionic liquid based hybrid materials, Chem. Soc. Rev. 40 (2011) 907–925, https://doi.org/10.1039/C0CS00059K.

[40] X. Sun, Y. Zhu, J. Zhu, K. Le, P. Servati, F. Jiang, Tough and ultrastretchable liquid-free ion conductor strengthened by deep eutectic solvent hydrolyzed cellulose microfibers, Adv. Funct. Mater. 32 (2022) 2202533, https://doi.org/10.1002/ADFM.202202533.

[41] X. Sun, Y. Zhu, Z. Yu, Y. Liang, J. Zhu, F. Jiang, Dialcohol cellulose nanocrystals enhanced polymerizable deep eutectic solvent-based self-healing ion conductors with ultra-stretchability and sensitivity, Adv. Sens. Res. (2023) 2200045, https://doi.org/10.1002/ADSR.202200045.

[42] M. Amjadi, K.U. Kyung, I. Park, M. Sitti, Stretchable, skin-mountable, and wearable strain sensors and their potential applications: a review, Adv. Funct. Mater. 26 (2016) 1678–1698, https://doi.org/10.1002/ADFM.201504755.

[43] D.S. Silvaraj, S. Bashir, M. Hina, J. Iqbal, S. Gunalan, S. Ramesh, K. Ramesh, Tailorable solid-state supercapacitors based on poly (N-hydroxymethylacrylamide) hydrogel electrolytes with high ionic conductivity, J. Energy Storage. 35 (2021), 102320, https://doi.org/10.1016/J.EST.2021.102320.

[44] L. Wu, Z. Chen, X. Ma, Chloride ion conducting polymer electrolytes based on cross-linked pmma-pp 14 cl-pp 14 tfsi ion gels for chloride ion batteries, Int. J. Electrochem. Sci. 14 (2019) 2414–2421. https://doi.org/10.20964/2019.03.49.

[45] D. Dobler, T. Schmidts, C. Zinecker, P. Schlupp, J. Schäfer, F. Runkel, Hydrophilic ionic liquids as ingredients of gel-based dermal formulations, AAPS PharmSciTech. 17 (2016) 923–931, https://doi.org/10.1208/S12249-015-0421-Y/TABLES/4.

[46] A. Soroudi, N. Hernández, J. Wipenmyr, V. Nierstrasz, Surface modification of textile electrodes to improve electrocardiography signals in wearable smart garment, J. Mater. Sci. Mater. Electron. 30 (2019) 16666–16675, https://doi.org/10.1007/s10854-019-02047-9.

[47] T. Pola, J. Vanhala, Textile electrodes in ECG measurement, in: Proc. 2007 Int. Conf. Intell. Sensors, Sens. Networks Inf. Process. ISSNIP, 2007: pp. 635–639. https://doi.org/10.1109/ISSNIP.2007.4496917.

[48] D. Pani, A. Achilli, P.P. Bassareo, L. Cugusi, G. Mercuro, B. Fraboni, A. Bonfiglio, Fully-Textile Polymer-Based ECG Electrodes: Overcoming the Limits of Metal-Based Textiles, Comput. Cardiol. (2010). 43 (2016). https://doi.org/10.22489/CinC.2016.109-460.

[49] D. Pani, A. Dessì, J.F. Saenz-Cogollo, B. Fraboni, A. Bonfiglio, G. Barabino, Fully textile, PEDOT : PSS based electrodes for wearable ECG monitoring systems, IEEE Trans. Biomed. Eng. 9294 (2015) 540–549, https://doi.org/10.1109/TBME.2015.2465936.

[50] T. Kelly, B.M. Ghadi, S. Berg, H. Ardebili, In Situ Study of Strain-Dependent Ion Conductivity of Stretchable Polyethylene Oxide Electrolyte, Sci. Reports 2016 61. 6 (2016) 1–9. https://doi.org/10.1038/srep20128.

[51] M. Moreno, R. Quijada, M.A. Santa Ana, E. Benavente, P. Gomez-Romero, G. González, Electrical and mechanical properties of poly(ethylene oxide)/intercalated clay polymer electrolyte, Electrochim. Acta. 58 (2011) 112–118, https://doi.org/10.1016/J.ELECTACTA.2011.08.096.

[52] E. Quartarone, P. Mustarelli, A. Magistris, PEO-based composite polymer electrolytes, Solid State Ionics. 110 (1998) 1–14, https://doi.org/10.1016/S0167-2738(98)00114-3.

[53] P.A. Haddad, Flexible film and breathable textile electrodes for electrodermal activity monitoring, The University of British Columbia, 2018.